UNIVERSIDADE DE SÃO PAULO

INSTITUTO DE FÍSICA
CAIXA POSTAL 20516
01498 SÃO PAULO - SP
BRASIL

PUBLICAÇÕES

IFUSP/P-987

HYPERON POLARIZATION IN A HYDRODYNAMICAL MODEL

Yogiro HAMA
Instituto de Física, Universidade de São Paulo

Takeshi KODAMA
Centro Brasileiro de Pesquisas Físicas
Rio de Janeiro, RJ, Brasil

Junho/1992

Hyperon Polarization in a Hydrodynamical Model

Yogiro HAMA

Instituto de Física, Universidade de São Paulo

São Paulo, Brasil

and

Takeshi KODAMA

Centro Brasileiro de Pesquisas Físicas

Rio de Janeiro, Brasil

ABSTRACT

A possible coherent origin of polarization phenomena in baryon production is suggested. By describing in terms of an optical potential the interaction of the hadronic matter in expansion with a baryon produced in its interior, the main features of the hyperon polarization observed in high energy hadronic collisions are shown to be well reproduced. In contrast to the existent models, this one can provide a natural explanation for the anti-hyperon polarization and may complement the usual quark-rearrangement mechanism in the case of hyperons.

PACS numbers: 13.85.Ni, 13.88.+e, 12.40.eE, 12.90.+b

In high-energy proton-proton or proton-nucleus collisions with hyperon (or anti-hyperon) production,

$$p + A \to Y(\overline{Y}) + X \quad , \tag{1}$$

where $Y = (\Lambda, \Sigma, \Xi)$, these particles appear to be significantly polarized [1-4]. This is a remarkable fact, because from a simple extrapolation of low-energy data as well as two-final-particle-collision data, we would expect that the hadronic interaction becomes less and less spin dependent as the incident energy increases. Thus, before the appearence of the hyperon polarization data, it was believed that hadron polarization is a low-energy phenomenon.

Some models have been proposed such as the semiclassical string model [5], the parton recombination model [6] and the Reggeized one-pion-exchange model [7], all of them essentally based on a mechanism of flavour recombination of the incident proton. All these models are found to reproduce the main characteristics of the hyperon polarization data, but they seem to meet trouble with the recently reported anti-hyperon data [3,4], since anti-hyperons have nothing in common with the proton and cannot be produced by a quark recombination.

In this work, we propose an alternative or complementary explanation by which the polarization appears as a consequence of a coherent interaction of the produced particle (we shall call it as such although it may just be a proto-particle or a group of constituents with correct quantum numbers, which eventually evolves into the observed particle) with the background hadronic matter. In such a picture, what is relevant is not the incident energy but the relative energy of the produced hyperon with respect to the hadronic matter, so that the polarization still appears as a relatively low-energy phenomenon. Also, as far

as the polarization is concerned, the specific character of the incident particle does not play any role except, perhaps, its initial energy. Thus, there is no *a-priori* restriction for anti-hyperons, which may be polarized as well.

To illustrate the idea, consider a simplified picture of an outgoing particle of momentum $\vec{k}$ emerging from a sharp surface of background hadronic matter. By making an analogy with optics, we shall represent the interaction by a complex potential $V = V_1 + iV_2$, inside the matter and $V = 0$ outside.

Writing the Dirac equation for our hyperon

$$E\Psi = (-i\vec{\alpha}\cdot\vec{\nabla} + \beta m + V)\Psi \ , \tag{2}$$

we have (see Fig. 1 for definitions of variables)

$$\begin{cases} \Psi_I(\vec{r}) = u_{in}(\vec{k}_{in})\ e^{i\vec{k}_{in}\cdot\vec{r}} + u_{ref}(\vec{k}_{ref})\ e^{i\vec{k}_{ref}\cdot\vec{r}} \ , \\ \Psi_{II}(\vec{r}) = u(\vec{k})\ e^{i\vec{k}\cdot\vec{r}} \ , \end{cases} \tag{3}$$

where the continuity of the wavefunction leads to

$$\vec{k}_{in} = \begin{pmatrix} k_1 \\ 0 \\ k_3' \end{pmatrix} \ , \ \vec{k}_{ref} = \begin{pmatrix} k_1 \\ 0 \\ -k_3' \end{pmatrix} \ , \ \vec{k} = \begin{pmatrix} k_1 \\ 0 \\ k_3 \end{pmatrix} \ . \tag{4}$$

Solving the Dirac equation, we express the spinor of the transmitted wave in the form

$$\begin{pmatrix} u^+(\vec{k}) \\ u^-(\vec{k}) \end{pmatrix} = \begin{pmatrix} T^{++} & T^{+-} \\ T^{-+} & T^{--} \end{pmatrix} \begin{pmatrix} u_{in}^+(\vec{k}_{in}) \\ u_{in}^-(\vec{k}_{in}) \end{pmatrix} \ , \tag{5}$$

where $+$ and $-$ represent, respectively, positive and negative polarizations normal to the collision plane (x_2 axis). We verify that $T^{+-} = T^{-+} = 0$, due to the continuity of the wavefunction.

Then, the transverse polarization P (parallel to x_2 axis) is written as

$$P = \frac{|T^{--}|^2 - |T^{++}|^2}{|T^{--}|^2 + |T^{++}|^2} \ , \tag{6}$$

where T^{++} and T^{--} may easily be computed as

$$\begin{aligned} T^{++} &= \frac{2\sqrt{2m(E+m)}N_+k_3'}{(E-V+m)k_3 + (E+m)k_3' - iVk_1} \ , \\ T^{--} &= \frac{2\sqrt{2m(E+m)}N_-k_3'}{(E-V+m)k_3 + (E+m)k_3' + iVk_1} \ , \end{aligned} \tag{7}$$

with the normalization constants $N_\pm$ given by

$$|N_\pm|^2 = \frac{|E-V+m|^2}{2\{m(E-V_1+m) + V_2^2 - (\mathrm{Im}\,k_3' \pm k_1)\mathrm{Im}\,k_3'\}} \ . \tag{8}$$

Physically, the polarization appears in our picture due to the well known spin-orbit interaction which, in the low-energy limit, writes $\hat{\vec{\sigma}}\cdot\vec{\nabla}V\times\hat{\vec{k}}/4m^2$. In our case, this term is effective only at the surface of the matter.

For unpolarized incident beam, one sees from Eqs.(6-8) that the net polarization of the outgoing flux is nonzero if the potential V contains an imaginary part ($V_2 \neq 0$). It is found that the sign of the polarization is the same as that of V_2. We also find that, if the potential contains positive real part, the polarization effect is enhanced and, for negative real part, it is reduced. In Fig. 2, we show how the transverse polarization varies as a function of the refraction angle θ for a pure imaginary potential. As seen there, larger polarization is produced for larger refraction angle, apparently in accordance with the observed larger polarization for larger values of the Feymann x_F variable. Since the polarization effect we discuss is due to the discontinuity in the potential V, we also expect that it increases with p_T, because such particles can leave the hadronic matter more easily and thus polarized,

whereas low-k_T particles may not have enough time to escape from the medium, so frozen out unpolarized in this case.

In order to incorporate the above mechanism into a more realistic situation, let us consider a longitudinally expanding cylindrical hadronic matter with transverse radius R. We shall parametrize the rapidity distribution of the collective flow by a Gaussian

$$\frac{d\rho}{dy_{fluid}} \propto e^{-\alpha y^2_{fluid}} \tag{9}$$

and assume that the matter density is constant in the transverse directions. Then, by making a naive assumption that the previous results embodied by (2) through (8) remain valid in each rest frame of the matter and that particles are produced in equilibrium at certain temperature T, the overall polarization is written as a convolution of the flow distribution (9) and the partial polarization given by (6), with an appropriate Boltzmann factor $\exp(-E/T)$ and normalization.

The interaction of our baryon with the background matter depends indeed on the matter density, giving rise to a time-varying potential. For the present estimate, we shall replace such a potential just by a time averaged value. However, there is one effect that we have explicitly to take into account, namely, the freezeout of the fluid. Since our particle is polarized only when it leaves the matter surface, it will remain unpolarized if the medium becomes rarefied before such an escape occurs. Writing the time interval during which our polarization mechanism is effective by Δt, the number of polarized baryons is

$$F_{pol} \propto 2\pi R \Delta t \frac{k_T}{E} , \tag{10}$$

whereas the one for unpolarized baryons is

$$F_{unpol} \propto \pi R^2 . \tag{11}$$

So, the net polarization shall be computed by taking these weights into account and, as a function of the particle momentum $\vec{k}$, reads

$$P(\vec{k}) = \frac{\int d\bar{y}\ P(k) F_{pol}\ e^{-\alpha(y-\bar{y})^2} E\ e^{-E/T}}{\int d\bar{y} (F_{unpol} + F_{pol})\ e^{-\alpha(y-\bar{y})^2}\ E\ e^{-E/T}} , \tag{12}$$

where $y = y(\vec{k})$ is the center-of-mass rapidity of the particle ($\bar{y}$ is the value relative to the fluid element) and $E = E(\vec{k}, \bar{y})$ the energy of the particle in the rest frame of the fluid element.

In the present picture, the polarization emerges as a result of the coherent interaction of the produced particle with the surrounding hadronic matter. Thus, such a mechanism should be more effective in the central region, whereas in the fragmentation region, some quark-recombination mechanism [5-7] could be dominant. Our model is also applicable for anti-baryons, which cannot be produced by a recombination from the incident proton. In this sense, it would be nice if we could compare the model with anti-hyperon data. However, due to the scarceness of such data, we choose the Ξ particles to illustrate how our model works. For Ξ particles the recombination mechanism is likely to be rather ineffective because of the increase of the strangeness quantum number by 2.

In Figs. 3-6, the polarization of Ξ^- in the reaction $p + Be \rightarrow \Xi^- + X$ calculated with the present model is compared to corresponding data. In this calculation, we used as input $\alpha = .5$, $V_1 = 0.7$ GeV, $V_2 = -0.5$ GeV, $T = 0.15$ GeV, $R/\Delta t = 2.5$. We see the results are quite satisfactory reproducing the main qualitative and quantitative features of the experimental data. We can also see that the data for $\bar{\Xi}^+$ are consistent with these calculations. The above values of α, T and $R/\Delta t$ are also consistent with the usual hydrodynamical picture of the multiparticle production process. In fact, the value of α determined by the inclusive rapidity distribution is around 0.5.

In our picture, the polarization is produced at the surface of the matter and it decreases slowly for large-k_T values. On the other hand, a low-k_T hyperon hardly leaves the matter before the freezeout, so its net polarization becomes reduced too. As a result, there appears a maximum of $|P|$ around 0.8 GeV. Looking at Fig. 6, it seems that this value is too small,when compared to data. However, if we include the transverse expansion of the fluid, such a minimum is expected to shift toward a higher-k_T value ($k_T \simeq 1.3\,\mathrm{GeV}$) [8], improving the agreement.

In the present simplified version, the potential $V = V_1 + \mathrm{i}V_2$ represents the effective interaction of the particle with the hadronic matter (including its absorption or creation) and it may vary from one particle to another. If we take $V_1 \simeq 1$ GeV and $V_2 \simeq -1$ GeV, the Λ-particle data are well reproduced, provided that the transverse momentum k_T and x_F are not so large ($k_T \lesssim 1.5$ GeV and $x_F \lesssim 0.5$). High-k_T particles are more likely to be produced by a hard collision process and so are probabaly out of the scope of the hydrodynamical description on which our model is based.

For Σ particles, the observed polarization data show an oposite sign compared to those of Λ and Ξ. In our model, this property is achieved with a positive V_2. In fact, taking $V_2 \simeq 1.0$ GeV, the correct sign and the magnitude of Σ polarization can be obtained. The positive imaginary part of the potential seems to imply that these particles be produced more in the surface region of the matter.

In sumary, the present simple calculations show that the polarization of hyperons, except in situations such that the quark recombination of the incident particle becomes dominant, can naturally be explained as due to a coherent interaction of the particle

with the background hadronic matter. This picture is particulary interesting for the anti-hyperon case. More data are desirable for antihyperon polarization.

The authors are grateful for the members of the Working Group on Hadron Interaction, especially, M.Betz and E.Veit for the stimulating discussions. This work has partly been supported by the Fundação de Amparo de Pesquisa do Estado de São Paulo (FAPESP). T.K. acknowledges the hospitality and the financial support given by USP, during his stay as a visiting fellow.

References:

[1] G. Bunce *et al.*, *Phys. Rev. Lett.* **36**, 1113 (1976); S. Erhan *et al.*, *Phys. Lett.* **82B**, 301 (1979); K. Heller *et al.*, *Phys. Lett.* **68B**, 480 (1977) and *Phys. Rev. Lett.* **41**, 607 (1978).

[2] C. Wilkinson *et al.*, *Phys. Rev. Lett.* **46**, 803 (1981); L. Deck *et al.*, *Phys. Rev.* **D28**, 1 (1983); K. Heller *et al.*, *Phys. Rev. Lett.* **51**, 2025 (1983); Y. W. Wah *et al.*, *Phys. Rev. Lett.* **55**, 2551 (1985); R. Ramerika *et al.*, *Phys. Rev.* **D33**, 3172 (1986); E. C. Dukes *et al.*, *Phys. Lett.* **193B**, 135 (1987); J. Duryea *et al.*, *Phys. Rev. Lett.* **67**, 1193 (1991).

[3] P. M. Ho *et al.*, *Phys. Rev. Lett.* **65**, 1713 (1990); *Phys. Rev.* **D44**, 3402 (1991).

[4] E761 collab., A. Morelos, "Polarization Mesurements of Σ^+ and $\overline{\Sigma^+}$", APS meeting, Washington, Apr/1991.

[5] B. Andersson, G. Gustafson and G. Ingelman, *Phys. Lett.* **85B**, 417 (1979).

[6] T. A. DeGrand and H. I. Miettinen, *Phys. Rev.* **D24**, 2419 (1981).

[7] A. V. Turbiner, *JETP Lett.* **22**, 182 (1975); J. Soffer and N. A. Törnqvist, *Phys. Rev. Lett.* **68**, 907 (1992).

[8] Y. Hama and F.S. Navarra, *Z. Phys.* **C 53**, 501 (1992).

Figure Captions:

Fig. 1: An incident wave in the matter (I) with $\vec{k}_{in}$ is partially reflected at $x_3 = 0$ and partially transmitted to the vacuum (II).

Fig. 2: Polarization of Ξ^- hyperon, P_{Ξ^-}, computed by using (6) as a function of the refraction angle θ. The potential has been chosen $V = -.3\,i$ GeV and the outgoing momentum $k_{\Xi^-} = 1$ GeV.

Fig. 3: Polarization of Ξ^- hyperon P_{Ξ^-}, calculated as a function of x_F at $p_{lab} = 400$ GeV for three values of k_T, is compared with data [2, 3]. The latter are classified in three k_T intervals: 0.4 GeV$< k_T <$ 0.55 GeV ($\triangle$); 0.7 GeV$\leq k_T <$ 1.0 GeV ($\blacksquare$); and 1.0 GeV$\leq k_T <$ 1.3 GeV ($\bigcirc$).

Fig. 4: Polarization of Ξ^- hyperon P_{Ξ^-}, calculated as a function of k_T at $p_{lab} = 400$ GeV for three values of x_F, is compared with data [2, 3]. The latter are classified in three x_F intervals: $0.2 < x_F \leq 0.4$ ($\triangle$); $0.4 < x_F \leq 0.6$ ($\blacksquare$); and $0.6 < x_F \leq 0.8$ ($\bigcirc$).

Fig. 5: Polarization of Ξ^- hyperon P_{Ξ^-}, calculated as a function of x_F at $p_{lab} = 800$ GeV for three values of k_T, is compared with data [2, 3]. The symbols are the same as in Fig. 3. $\bar{\Xi}^+$ data have also been included here ($\square$).

Fig. 6: Polarization of Ξ^- hyperon P_{Ξ^-}, calculated as a function of k_T at $p_{lab} = 800$ GeV for three values of x_F, is compared with data [2, 3]. The symbols are the same as in Fig. 4. $\bar{\Xi}^+$ data have also been included here: $0.2 < x_F \leq 0.4$ ($\blacktriangle$) and $0.4 < x_F \leq 0.6$ ($\square$).

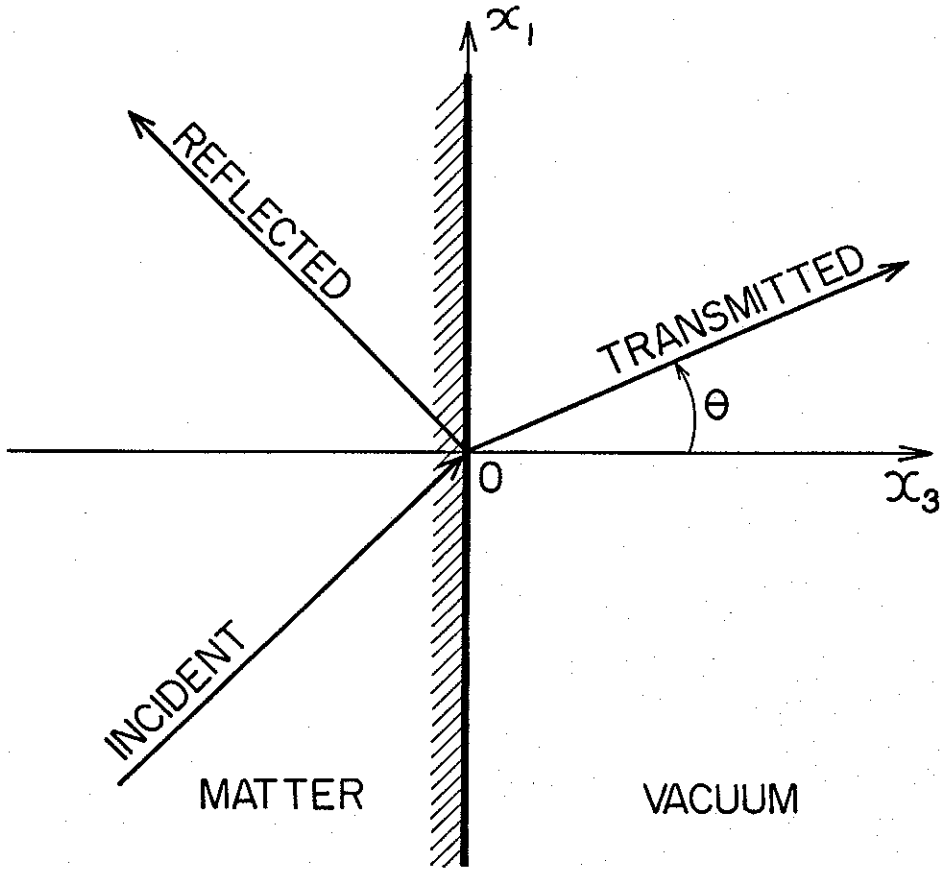
x_1
REFLECTED
TRANSMITTED
θ
0
x_3
INCIDENT
MATTER
VACUUM

Fig. 1

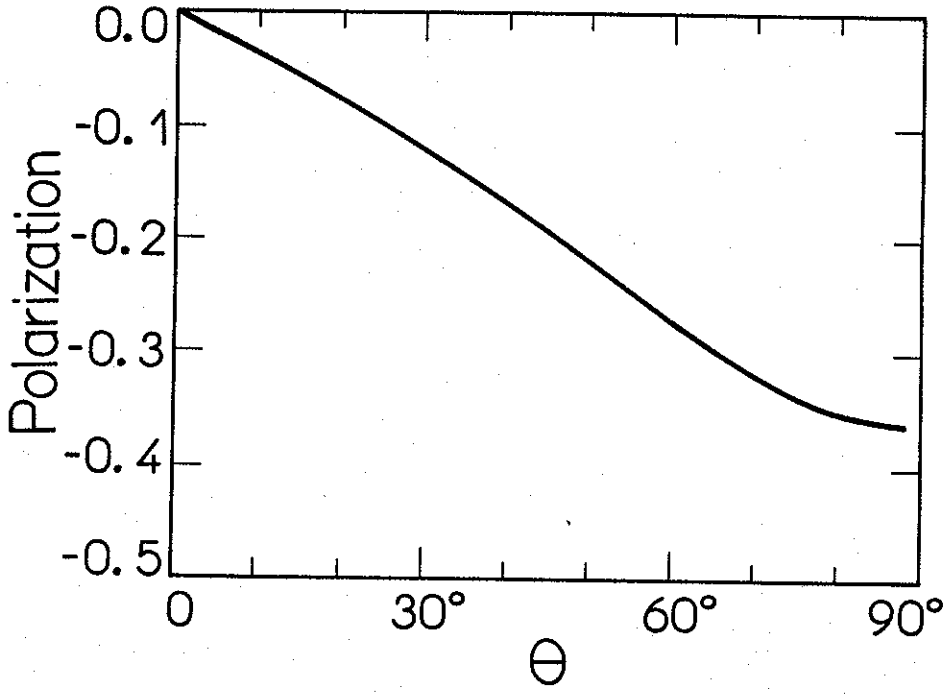
0.0
-0.1
-0.2
-0.3
-0.4
-0.5
Polarization
0
30°
60°
90°
θ

Fig. 2

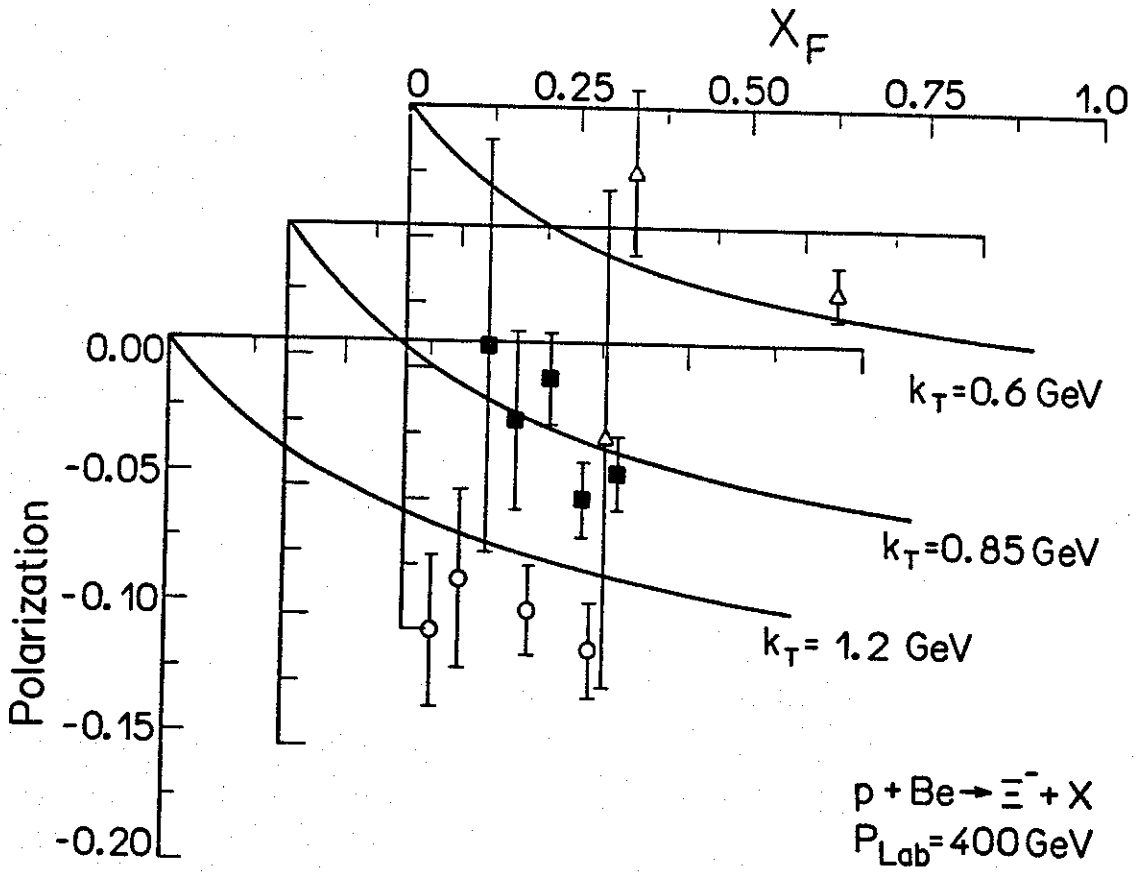
X_F
0
0.25
0.50
0.75
1.0
0.00
-0.05
-0.10
-0.15
-0.20
Polarization
k_T=0.6 GeV
k_T=0.85 GeV
k_T= 1.2 GeV
p + Be → Ξ⁻ + X
P_{Lab}=400 GeV

Fig. 3

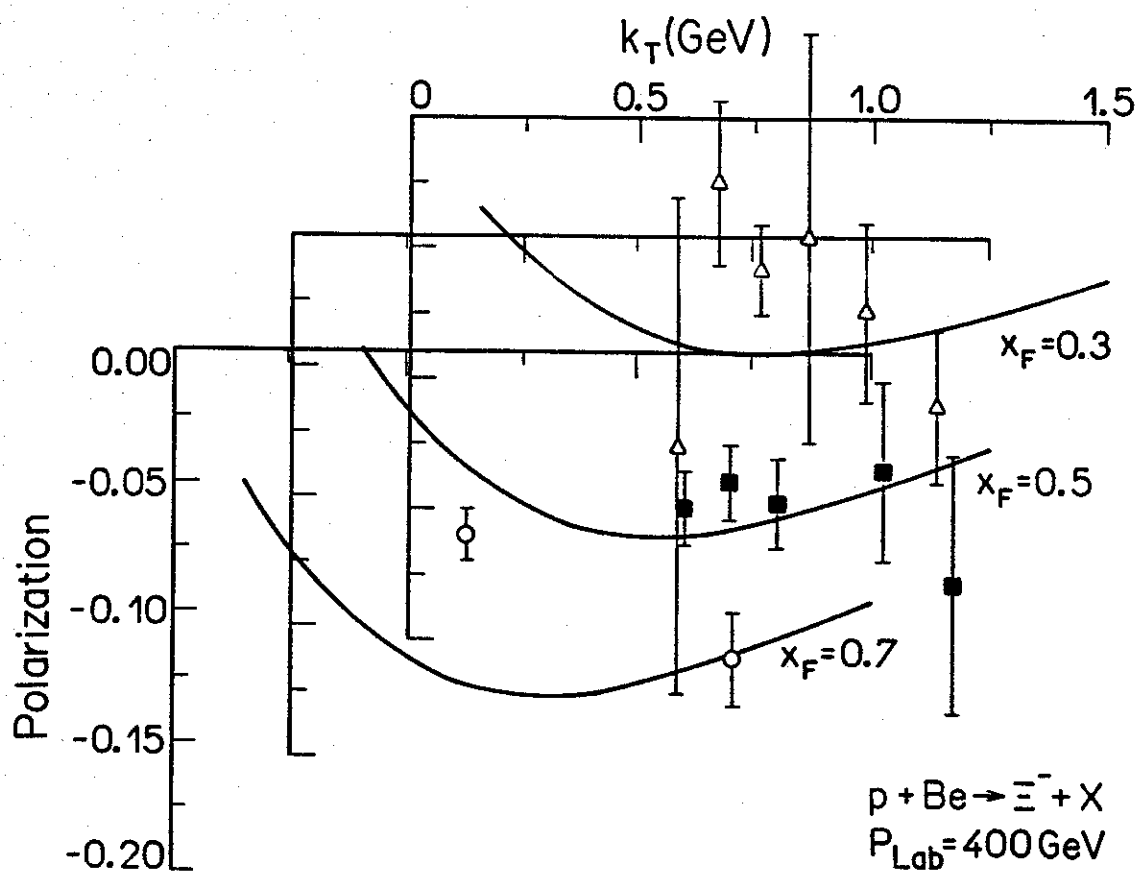
k_T(GeV)
0
0.5
1.0
1.5
0.00
-0.05
-0.10
-0.15
-0.20
Polarization
x_F=0.3
x_F=0.5
x_F=0.7
p + Be → Ξ⁻ + X
P_{Lab}=400 GeV

Fig. 4

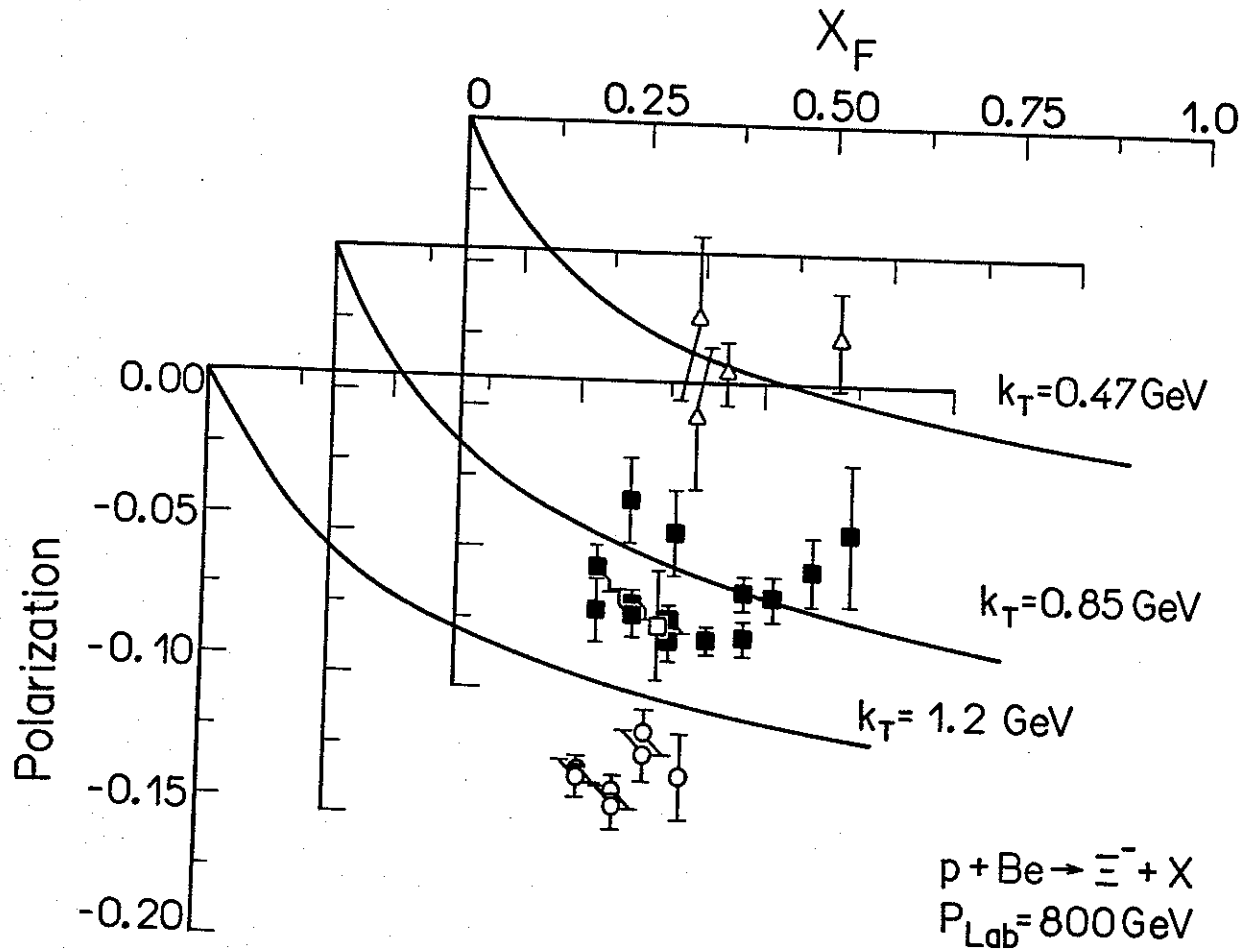
X_F
0
0.25
0.50
0.75
1.0
0.00
-0.05
-0.10
-0.15
-0.20
Polarization
k_T=0.47 GeV
k_T=0.85 GeV
k_T= 1.2 GeV
p + Be → Ξ⁻ + X
P_{Lab}= 800 GeV

Fig. 5

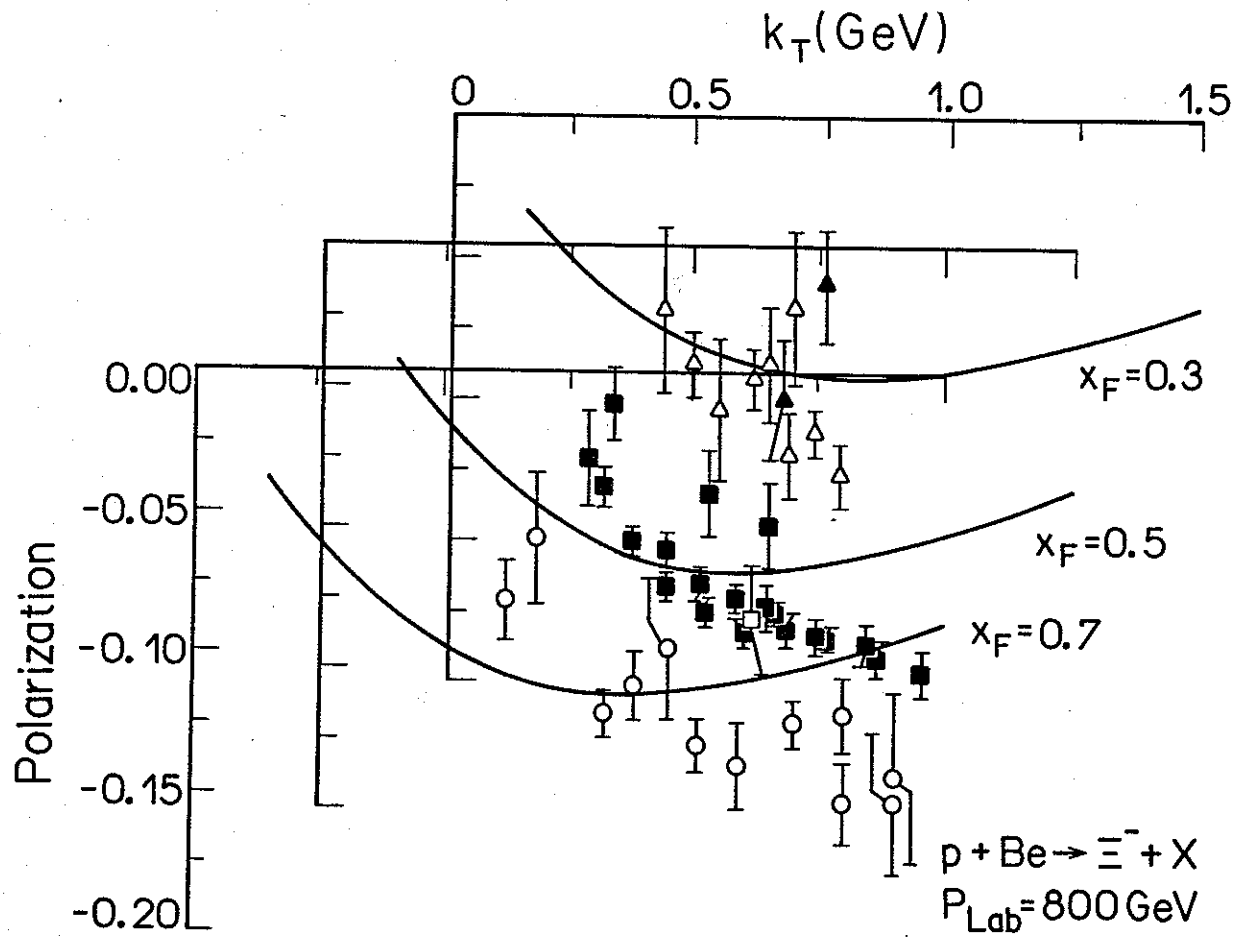
k_T(GeV)
0
0.5
1.0
1.5
0.00
-0.05
-0.10
-0.15
-0.20
Polarization
x_F=0.3
x_F=0.5
x_F=0.7
p + Be → Ξ⁻ + X
P_{Lab}= 800 GeV

Fig. 6